ISSN 1392 – 1231. CHEMINĖ TECHNOLOGIJA. 2009. Nr. 1 (50)

Contribution of spark plasma sintering to the development of mullite–ZrO_2 ceramics

I. Sperberga, G. Sedmale, A. Pludons, A. Hmelov
Institute of Silicate Materials, Riga Technical University,
Azenes str. 14/24, LV-1048 Riga, Latvia
E-mail: sperberga@ktf.rtu.lv

I. Steins
Institute of Inorganic Chemistry, Riga Technical University,
Miera str. 34, LV-2169 Salaspils, Latvia

Received 5 February 2009; Accepted 17 February 2009

Spark Plasma Sintering (SPS) of the two kinds of powder compositions of γ-Al_2O_3, SiO_2–gel, ZrO_2 and Y_2O_3 with and without mineralizer – illite clay and prepared by milling in a planetary ball mill was performed. Investigations were carried out in order to show the influence of this sintering method on the phase development and some properties of sintered ceramic samples. It is shown that submicronic powder has enabled to obtain a sample with a relative density of up to 98–100% at temperatures starting from 1200 °C for samples without an illite clay additive and at 1150 °C with this additive.

SPS sintering led to the formation of mullite and ZrO_2 cubic as the main phases. No development of corundum and zirconia (tetr.), as it was established in conventionally sintered samples, using SPS was observed.

Introduction

Mullite ($3Al_2O_3 \cdot 2SiO_2$) has become a promising candidate for high-temperature structural applications in an oxidizing atmosphere due to its unique combination of advantageous properties such as low thermal expansion, high creep resistance, excellent oxidation resistance and high-temperature strength, low density [1–4]. However, monolithic mullite bodies suffer from low values of bending strength and fracture toughness [5].

On the other hand, composite materials containing zirconia (ZrO_2) are extensively studied because of the martensitic phase transformation of zirconia under applied stress which contributes considerably to the mechanical properties of ceramics [6–9]. ZrO_2 has superior physical and mechanical properties including high hardness, wear resistance, elastic modulus and high melting temperature, whid make it attractive as a structural engineering material [10].

The spark plasma sintering (SPS) technique has been undergoing a fast development since the beginning of the 1990s thanks to its extremely high sintering rate. Originally born in Asia, this technique is now spreading in the Western countries. SPS is a versatile technique used for a rapid densification of material at moderate temperatures [11–14]. Spark plasma sintering has several advantages over pressurless sintering, including lower sintering temperatures and shorter keeping times. Spark plasma sintering techniques have been extensively used to produce a wide range of materials including metals, ceramics, glass and biomaterials, etc. [15–20]. The fast heating rate makes it unique for investigating bulk nano materials since the nano-scale structure may be retained due to the rapid sintering cycle. A fully dense material may be sintered within minutes using SPS instead of hours when conventional methods are used.

The present work is related to the study of shrinkage, phase development and morphology of mullite-zirconia ceramics obtained by spark plasma sintering.

Materials and methods

Six powders (A, C, D, E, F and G) were prepared from starting synthetic materials of chemical grade – γ-Al_2O_3 obtained from $Al(OH)_3$ by heating at 550 °C for 1 h, SiO_2 gel, ZrO_2 and Y_2O_3. As an additional component, a mineral raw material – illite clay – was used in powders C, G and E. The starting powder mixtures were prepared by the ball-milling process in a planetary laboratory mill with corundum balls. Powders were milled for 4 h (A and C), for 12 h (F and G) and for 24 h (D and E).

The particle size of powders was determined with a zeta potencial analyser s/n 21386. In the powders particles with the average size of 150–350 nm prevailed.

The phase composition of sintered samples was analysed using XRD (model Rigaku, Japan, with CuK_α radiation at a scanning interval from 2θ = 10–60° and speed 4 °/min.).

Atomic force microscopy measurements were performed with a scanning probe microscope *VEECO SPM II* (USA).

The powder mixtures were sintered in an SPS apparatus in which the cylindrical samples are 20 mm in diameter and about 5 mm in height, at temperatures varying between 1150 and 1400 °C with a keeping time of 2 min. The heating rate was 100 °C/min under a pressure of 30 MPa. The vacuum level of 6 Pa was maintained during the SPS process. For this work, an SPS apparatus (Sumimoto, Model SPS – 825.CE, Dr. Sinter, Japan) was used.

The bulk density and the relative density or densification of the sintered samples was tested by the Archimedes method, using a distilled water medium.

Results and discussion

The study shows that the parameter controling at the first order the sintering temperature range is the initial grading of powder. This is obvious when comparing the shrinkage associated to the sintering of the powders A, C (milled for 4 h), F, G (milled for 12 h) and D, E (milled for 24 h) (Figs. 1 and 2).

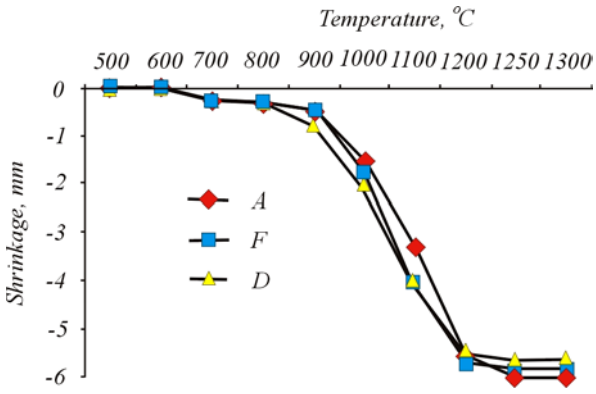

Fig. 1. Shrinkage of the powders A, F and D (without illite clay additive)

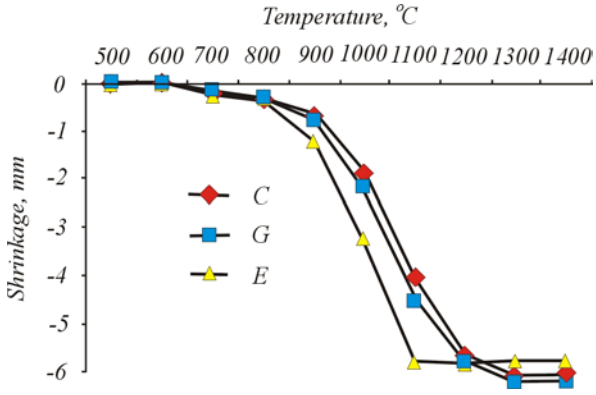

Fig. 2. Shrinkage of the powders C, G and E (with illite clay additive)

Following the linear shrinkage curves versus temperature, the shrinkage starts at 600 °C in all powders. Differences the in shrinkage of all samples appear at 800 °C when, as expected, the specific surface area of different powders starts to play the main role in the sintering mechanism under SPS conditions and a smaller grain size contributes to shifting the sintering towards "the low temperature" domain. Comparing the shrinkage of samples prepared from powders with and without clay additive, there is some difference in temperatures when the values of shrinkage are nearly the same. A sample obtained from powder E (with illite clay) reaches the maximum shrinkage at 1100 °C and is by approximately 100 °C lower than for a sample obtained from powder D (without illite clay).

Figure 3 shows the atomic force microscopy images of samples (after spark plasma sintering) obtained from powders milled for different time. AFM shows that materials with the grain size in a nanometer scale (varying within 40–195 nm depending on the starting powder) are obtained in SPS.

X-ray diffraction patterns reveal only peaks typical of mullite and zirconia with some traces of quartz in all samples obtained at 1250 °C (Fig. 4). Very similar XRD patterns were obtained in this case, possibly because in artificial mullite–zirconia forming systems, alongside Al_2O_3 and SiO_2 as the main components, also components contributing to the development of mullite and zirconia are present. Evidently this component (in this case Y_2O_3) promotes the diffusion or transfer of alumina and silica structural motives on the formed nuclei of the mullite crystalline phase as well as the formation of zirconia (cubic). In spite of the fact that powders were milled for different time and some of them contained a clay additive, an equal development of mullite and zirconia in all samples occurred in the same conditions. XRD diffraction patterns of sample F (milled for 12 h) obtained at different temperatures by SPS show that with decreasing the sintering temperature, the intensity of zirconia (cubic) decreases as well, and instaed of zirconia (cubic) there appears baddeleyite, another modification of zirconia. Also, an increase of quartz phase intensity in a sample obtained at 1150 °C is observed.

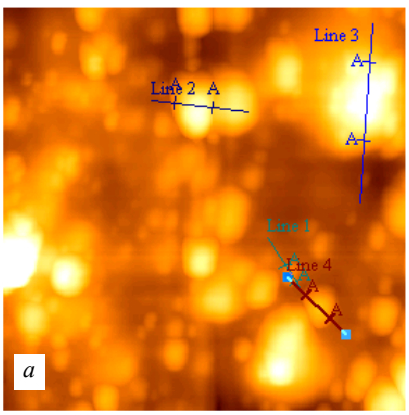

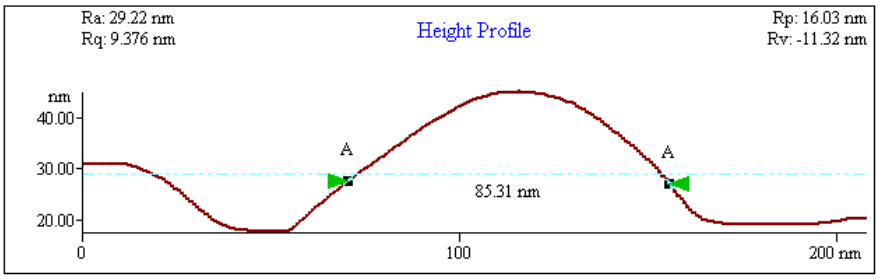

	Arc length	Bearing Ratio	Bearing Ratio	Peak (Rp)	Valley (Rv)	Cursor
Line 1	1.579 µm	@30.0% 25.26 nm	@80.0% 19.55 nm	8.618 nm	-5.584 nm	A d: 49.47 nm
Line 2	1.638 µm	@30.0% 56.11 nm	@80.0% 24.15 nm	18.84 nm	-28.55 nm	A d: 92.71 nm
Line 3	1.884 µm	@30.0% 62.26 nm	@80.0% 14.53 nm	33.76 nm	-33.52 nm	A d: 194.2 nm
Line 4	**1.626 µm**	**@30.0% 34.66 nm**	**@80.0% 19.49 nm**	**16.03 nm**	**-11.32 nm**	**A d: 85.31 nm**

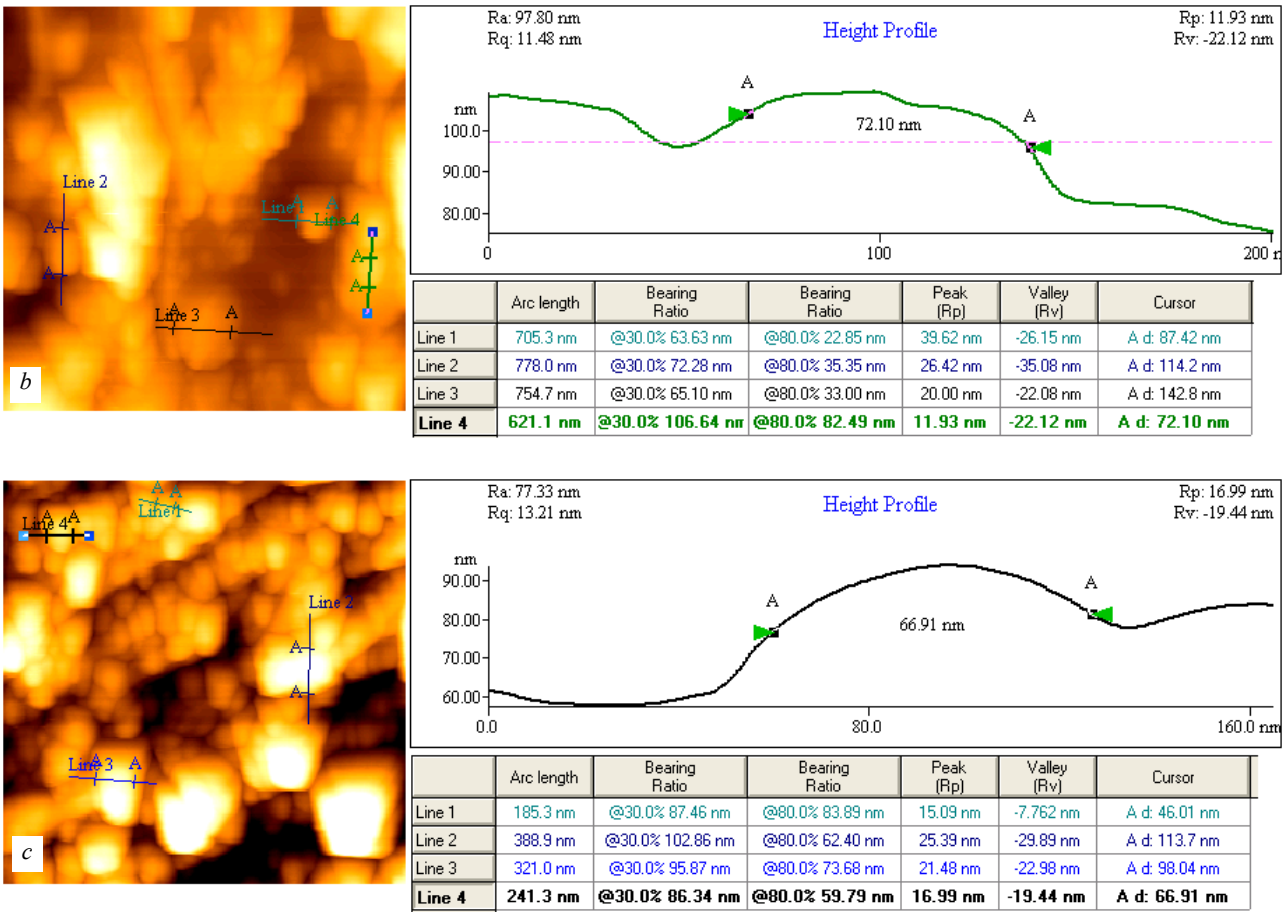

Fig. 3. Atomic force microscopy of samples: *a* – sample A (milled for 4 h); *b* – sample F (milled for 12 h) and *c* – sample D (milled for 24 h)

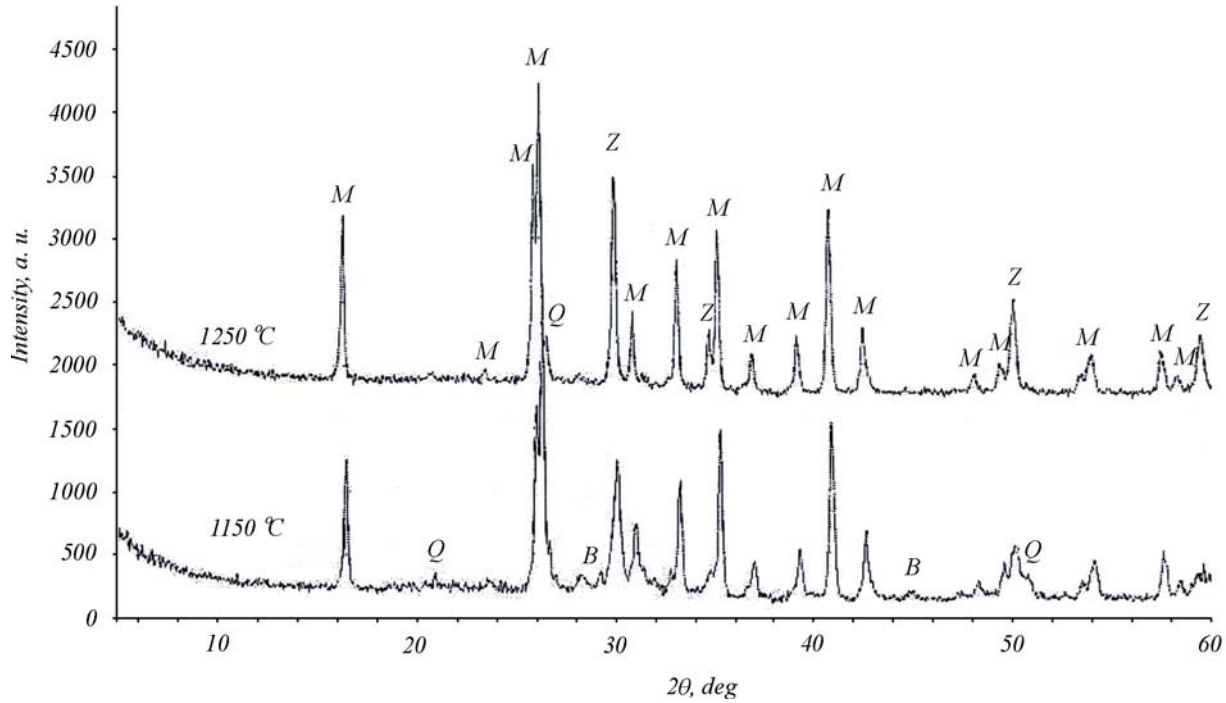

Fig. 4. Characterization by XRD of the sample F obtained by reactive sintering by the SPS technique at different temperatures: M – mullite, Z – zirconia (cub.), B – baddeleyite, Q – quartz

Figure 5 shows that densities for the obtained samples range from 2.5 up to 3.3 g/cm^3, which corresponds to the densification in the range 98–100%. Densities for samples A, F and D obtained from powders without a clay additive are slightly higher than for samples C, G and E containing a clay additive. For instance, powders F and G (both milled for 12 h before SPS) showed the densities of 3.20 and 2.70, respectively.

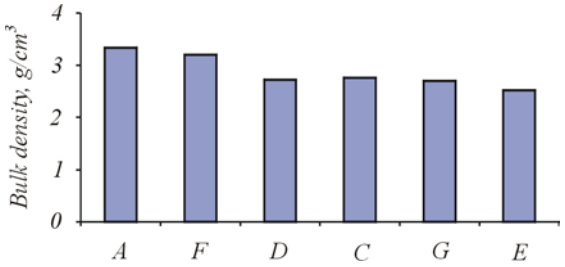

Fig. 5. Relationship between the bulk densities of different samples prepared at 1250 °C

On the other hand the effect of particle size of the starting powders on the density of samples obtained in SPS can be seen: the smaller the particle size of the starting powders, the higher the density under the same SPS conditions. Evidently, the particle size of the starting powders plays an important role in the spark plasma sintering process.

Conclusions

Formation of mullite–zirconia ceramic material from differently milled starting powders was achieved by spark plasma sintering (SPS). The applied SPS treatment induces reactions resulting in the formation of mullite and zirconia cubic at 1250 °C. AFM showed that materials with the grain size 40–195 nm (depending on the starting powder) were obtained using SPS. All materials were densified up to 98–100%. We concluded that the particle size of the starting powders plays an important role in the spark plasma sintering process.

References

1. **Aksay I. A., Dabbs D. B., Sarikaya M.** // J. Amer. Ceram. Soc. 1991. Vol. 74. P. 2343–2358.
2. **Rodrigo P. D., Boch P.** // J. High. Tech. Ceram. 1985. Vol. 1. P. 330–334.
3. **Sacks M. D., Bozkurt N., Scheiffele G. W.** // J. Amer. Ceram. Soc. 1991. Vol. 74. P. 2428–2437.
4. **Meng J., Cai S., Yang Z., Yuan Q., Chen I.** // J. Eur. Ceram. Soc. 1998. Vol. 18. P. 1107–1114.
5. **Rezaie H. R., Rainforth W. M., Lee W. E.** // J. Eur. Ceram. Soc. 1999. Vol. 18. P. 1177–1187.
6. **Kaberi D., Banerjee G.** // J. Eur. Ceram. Soc. 2000. Vol. 20. P. 153–157.
7. **Yaroshenko V., Wikinson D. S.** // J. Amer. Ceram. Soc. 2001. Vol. 84. P. 850–858.
8. **Mangalaraja R. V., Chandrasekhar B. K., Manohar P.** // Mater. Sci. Eng. 2003. A 343. P. 71–75.
9. **Kaya C., Kaya F., Marsoglu M.** // Mater. Sci. Eng. 1998. A 247. P. 75–80.
10. **Hannink R. H., Kelly P. M., Muddle B. C. //** J. Amer. Ceram. Soc. 2000. Vol. 3. P. 461–467.
11. **Tokita M.** // New Ceram. 1997. Vol. 10. P. 43–53.
12. **Mishra R. S., Risbud S. H., Mukherjee A. K.** // J. Mater. Res. 1998. Vol. 13. P. 86–89.
13. **Nygren M., Shen Z.** // Solid State Sci. 2003. Vol. 5. P. 125–131.
14. **Harada Y., Uekawa N., Kojima T., Kakegawa K.** // J. Eur. Ceram. Soc. 2008. Vol. 28. P. 235–240.
15. **Wan J. L., Duan R. G., Mukherjee A. K.** // Scripta Mater. 2005. Vol. 53. P. 663–667.
16. **Kim C. K., Lee H. S., Shin S. Y., Lee J. C., Kim D. H.** // Mater. Sci. Eng. 2005. A 406. P. 293–299.
17. **El-Eskandarany M. S., Omori A., Inoue A.** // J. Mater. Res. 2005. Vol. 20. P. 2845–2850.
18. **Shen B. L., Inoue A.** // J. Mater. Res. 2003. Vol. 18. P. 2115–2120.
19. **Anselmi-Tamburini U., Garay J. E., Munir Z. A.** // Scripta Mater. 2006. Vol. 54. P. 823–828.
20. **Chaim R.** // Mater. Sci. Eng. 2007. Vol. 443. P. 25–32.

I. Sperberga, G. Sedmale, A. Pludons, A. Hmelov, I. Steins

KIBIRKŠTINIO PLAZMINIO SUKEPINIMO METODO TAIKYMAS MULITO-ZrO_2 KERAMIKOS SINTEZEI

S a n t r a u k a

Kibirkštinis plazminis sukepinimas atliktas dviems, sumaltiems planetariniame rutuliniame malūne, miltelių mišiniams – γ-Al_2O_3, SiO_2-gelis, ZrO_2 ir Y_2O_3 su mineralizatoriumi – ilito moliu ir be jo. Tyrimai atlikti norint parodyti šio sukepinimo metodo įtaką mineralų susidarymui ir susidariusios (sukepusios) keramikos savybėms. Nustatyta, kad submikroskopiniai milteliai aptikti esant santykiniam tankiui iki 98–100 %, sukepinimą atlikus 1200 °C temperatūroje bandiniuose be ilito molio priedo ir 1150 °C temperatūroje su priedu.

Šio sukepinimo metodo metu pagrindinis susidaręs mineralas yra kubinis ZrO_2. Įprastinio sukepinimo metu korundas ir tetragoninis cirkonis nesusidarė.